Effect of Graphite Precursor Flake Size on Energy Storage Capabilities of Graphene Oxide Supercapacitors

S. Perumal, A.L.L. Jarvis, and M.Z. Gaffoor

Abstract— **In this research supercapacitors were fabricated using graphene oxide (GO) as the electrode material. GO was synthesized using natural graphite precursor with varying flake sizes. GO was characterized by High-Resolution Transmission Electron Microscopy (HRTEM), Elemental Analysis, Fourier Transform Infrared (FTIR) spectroscopy and Raman spectroscopy. Cyclic voltammetry was carried out at different scan rates to determine the specific capacitance and energy density of the electrode material. An increase in specific capacitance was seen with an increase in graphite precursor flake size. A specific capacitance and energy density of 204.22 $F.g^{-1}$ and 102.11 $kJ.kg^{-1}$ respectively at scan rate 10 $mV.s^{-1}$ was obtained for the GO sample synthesized from graphite precursor with an average particle size of 0.45 mm. This sample also had the highest specific capacitance for all scan rates.**

Index Terms— **Energy density, Flake size, Graphene oxide, Supercapacitor**

I. Introduction

ESKOM, South Africa's primary electricity provider, cannot meet the energy demand with their current non-renewable energy-based power plants [1]. In 2018, the Department of Energy pledged to get more renewable energy across the country, and especially to rural areas [2]. The intermittent nature of renewable energy sources, however, creates many challenges in energy storage. Therefore, there has been considerable interest in finding efficient energy storage devices for renewable energy [3]. A promising candidate is a supercapacitor due to its high power density, and excellent rate capability, which is desirable in energy storage devices [4]. There are other possible candidates that include batteries, fuel cells, and flywheels.

This promising candidacy of supercapacitors has resulted in the supercapacitor technology having undergone considerable research and development in recent years. Supercapacitors have a high power density and a low energy density as compared to lithium-ion batteries [5]. For supercapacitors to realize their potential, their energy density must be improved [6]. A meaningful way to address this is to develop advanced electrode materials. One of the unusual materials to use as the electrodes of the supercapacitor is graphene oxide (GO). GO acts as a cathode and separator in batteries due to its insulating nature thus avoiding short circuit in the battery [7]. GO has also been shown to improve battery performance [8] [9] [10] [11] [12].

GO is a two-dimensional (2-D) material made from oxidizing graphite. Graphene oxide research is important considering the abundance of carbon sources in South Africa. GO is hydrophilic meaning it is readily dispersible in water. Therefore, it is easy to work with, no expensive solvent or binders are required. GO was first reported as an electrode material for supercapacitors in 2011 by Bin Xu *et al.* [13]. GO had a specific capacitance of 189 $F.g^{-1}$, higher than that of graphene. This result was attributed by an additional pseudocapacitance effect of attached oxygen-functional groups on the basal plane [14]. In 2018, GO proved to be an excellent electrode material when combined with conductive electrode bulk ink with a specific capacitance of 423 $F.g^{-1}$ [15]. The properties of GO can be tailored by varying the graphite precursor used for synthesis. By using graphite precursors with different flake sizes, the size and structure of GO are affected [16]. Oxidation of GO is greater when graphite precursor with shorter crystallite sizes was used [17]. So if GO were synthesized with a graphite precursor of smaller flake size, it would be better oxidized and therefore have more oxygen functional groups. This more significant amount of oxygen functional groups would give more pseudocapacitance effect and therefore have a higher capacitance than GO synthesized from graphite precursor with larger flake size. When purchasing commercially available natural graphite, the only difference in

Based on "Effect of flake size of natural graphite precursor on graphene oxide supercapacitor for energy storage," by S. Perumal, A.L.L Jarvis and M. Z. Gaffoor which was published in the Proceedings of the SAUPEC/RobMech/PRASA 2020 Conference held in Cape Town, South Africa, 29-31 January 2020. © 2020 SAIEE.

This paper was submitted for review on 19 June 2020. This paper was submitted for re-review on 04 December 2020. This work was supported in part by Asbury Carbons and Eskom.

S. Perumal is with the School of Electrical, Electronic & Computer Engineering, University of KwaZulu-Natal, Durban, South Africa (e-mail: 214502296@stu.ukzn.ac.za).

A.L.L. Jarvis is with Eskom Power Plant Engineering Institute HVDC Centre, University of KwaZulu-Natal, Durban, South Africa (e-mail: jarvis@ukzn.ac.za).

M.Z. Gaffoor is with the School of Electrical, Electronic & Computer Engineering, University of KwaZulu-Natal, Durban, South Africa (e-mail: mohammedzaahidgaffoor@gmail.com).

choice of natural graphite is varying flake sizes.

In this paper, an investigation into the link between the flake size of the graphite precursor used to synthesize GO, and the energy storage characteristics of the GO supercapacitor is presented.

II. Background

A supercapacitor is an energy storage device with high surface area porous electrodes, and a thin dielectric (electrolyte) [18]. The interface between the electrolyte and the electrode is the electric double layer. The capacitances gained from this type of architecture are orders of magnitude higher than conventional capacitors. Supercapacitors are categorized as per Fig. 1, initially by the charge storage mechanism (type), thereafter, by the electrode material used, i.e. Electrochemical Double Layer Capacitor (EDLC) and GO respectively.

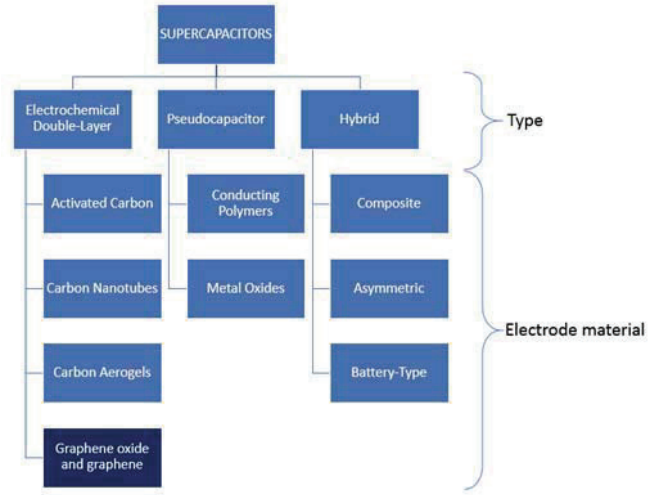

Fig. 1. Categorization of supercapacitors

EDLC's mechanism for storing charge is non-faradaic, which means charges are distributed on surfaces by physical processes that do not involve the making or breaking of chemical bonds [19]. The double-layer in name 'electrochemical double-layer capacitor' refers to the double layer of charge. One layer of charge accumulates on the electrode surface due to the voltage applied. The other layer of charge is the ions from the electrolyte that diffuse across the separator into the pores of the electrode of the opposite charge, as seen in Fig. 2. The capacitance gained from this mechanism is known as double-layer capacitance.

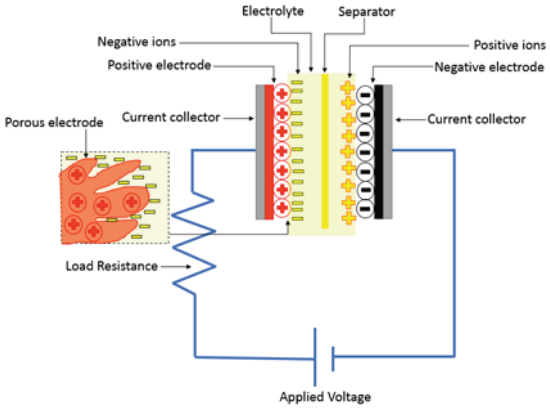

Fig. 2. Schematic diagram of supercapacitor showing EDLC

The capacitance of porous carbon materials like GO is mainly contributed by double-layer capacitance from electrostatic charge accumulation, and about 1-5 % is contributed by pseudocapacitance [20]. This pseudocapacitance comes from the high content of oxygen functional groups [21] which is inherent in GO. Pseudocapacitance charge storing mechanism is faradaic, unlike double-layer capacitance, and occurs as quick surface reduction and oxidation (redox) reactions.

The critical parameters for supercapacitors are specific capacitance, equivalent series resistance (ESR), energy density, and power density. Specific capacitance is the capacitance normalized by electrode mass (in grams), volume (in cm^3), or area (in cm^2). ESR is the internal resistance of the supercapacitor. Energy density is the amount of energy the supercapacitor can store and is presented as a specific energy density measured in $J.kg^{-1}$ [22]. The process in which supercapacitor stores its energy is shown in Fig. 3 demonstrated with a simple Gouy-Chapman Electric Double Layer Model [23] [24] (the second earliest supercapacitor model) of the supercapacitor. There are more recent complex supercapacitor models which include Bockris-Müller-Devanathan (BMD) model [25] formulated in 1963 by John O'Mara Bockris, a South African electrochemist together with Klaus Müller a German chemist, and Michael Angelo Vincent Devanathan a Sri Lankan chemist.

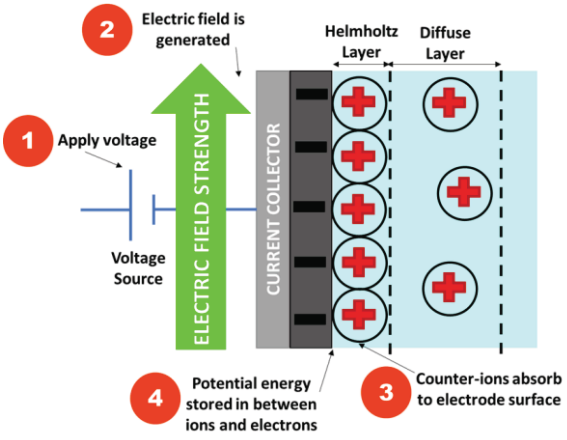

Fig. 3. Process of energy storage in supercapacitor

Obtaining the supercapacitor characteristics are most commonly done by cyclic voltammetry (CV). CV can be performed to evaluate capacitance of the as-prepared active electrode material GO and the operating voltage window of the electrolyte. CV is an analytical technique in which current produced via a redox reaction is monitored as a function of the scanned potential applied to an electrode [26]. The instrumentation used in CV analysis consists of a signal generator, potentiostat, working electrode (WE), reference electrode (RE), and counter electrode (CE). CV can either be done using a two-electrode system or three-electrode system [27]. Three-electrode system is accurate in controlling the voltage at the WE while measuring the current flowing from the WE to CE since it uses a RE that is ideally non-polarizable proving to be consistent and reliable [20]. Three-electrode system is also advantageous due to the quick electrode preparation.

Graphene oxide is synthesized from oxidizing graphite with a strong oxidizing agent such as potassium chlorate ($KClO_3$), and potassium permanganate ($KMnO_4$) [28]. GO has good wettability since it is hydrophilic which is a desirable property for supercapacitor electrode material [29] [30]. Having good wettability is essential for electrode materials in supercapacitors as it can soak up the electrolyte easily and thus improving ion transport within the supercapacitor. The structure of GO is a single sheet of graphite which is graphene with oxygen functional groups which include carbonyl, carboxyl and hydroxyl on the sheet edge, and epoxide on the basal plane as shown in Fig. 4 [31].

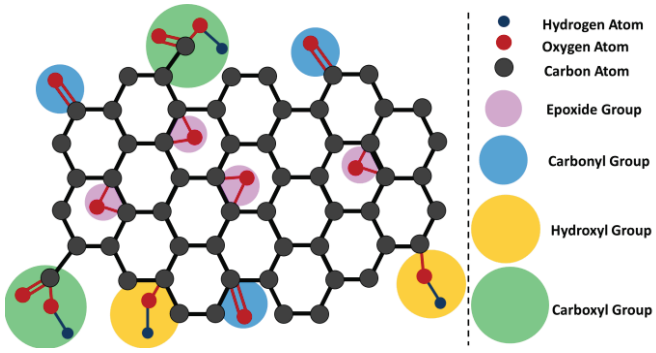

Fig. 4. Structure of GO showing carbonyl, carboxyl and hydroxyl on the sheet edge, and epoxide on the basal plane

III. Experimental

The GO supercapacitor is comprised of three parts viz. electrode material, current collectors, electrolyte. The current collector and electrolyte were kept constant for all samples, and the electrode material was varied.

A. Synthesis of GO

Four different graphite precursors from Asbury Carbons were used viz. Grade 230U, 3243, 3160, and 3061 which was called AN1-GO, AN2-GO, AN3-GO, and AN4-GO respectively for easy identification. The average particle sizes for AN1-GO, AN2-GO, AN3-GO, and AN4-GO are 0.045 mm, 0.105 mm, 0.1250 mm, and 0.4500 mm respectively. These graphite precursor average particle sizes were obtained from the graphite precursor datasheets received from Asbury Carbons. Graphite precursors were used as received. GO was synthesized by oxidizing the graphite precursor using the Hummers method with additional potassium permanganate [32]. The GO powders obtained at the end of the synthesis process is shown in Fig. 5.

Fig. 5. GO Samples (a) AN1-GO, (b) AN2-GO, (c) AN3-GO, (d) AN4-GO

B. Fabrication of current collectors

The design of the current collector was drawn using SolidWorks software, as shown in Fig. 6. The active electrode area on the stainless steel current collector, 24 mm x 24 mm, which was arbitrarily selected does match previously reported supercapacitor electrode sizes [33]. The current collectors were fabricated using stainless steel with 0.5 mm thickness. Symmetric current collectors were made by laser cutting. Stainless steel was chosen due to its low corrosion rate. This property is a requirement due to the use of an acidic electrolyte. Stainless steel has been used as a current collector in many commercially available supercapacitors.

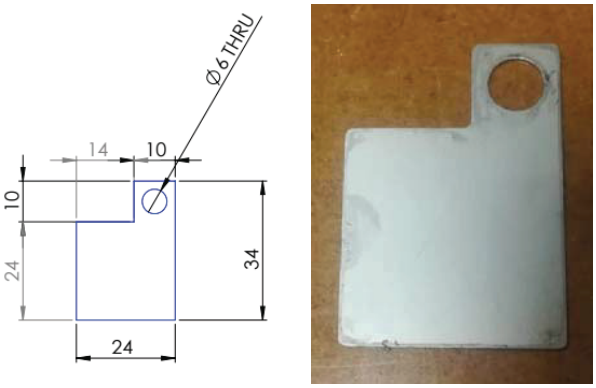

Fig. 6. Stainless steel current collector with dimensions

C. Preparation of GO electrode

GO solution with 0.1 %wt. concentration was made by adding 0.03 g of GO powder to 30 ml of deionized water. This concentration is considered to be low, and along with an initial 1-hour sonication and 10 minutes sonication before each coat, mitigated agglomeration of GO [34]. The solution was drop-casted onto stainless steel substrate (Fig. 7) and left to dry in air overnight at room temperature. In order to attain a homogenous GO deposit on the substrate, five separate individual coats were applied [34].

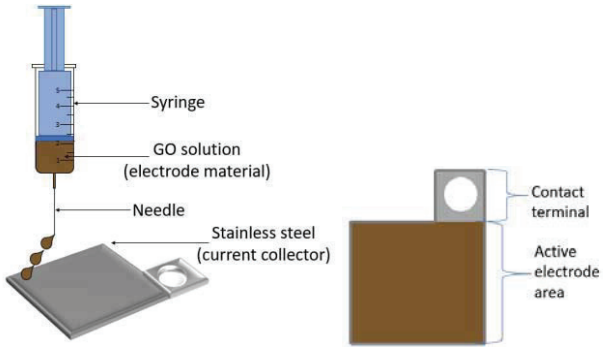

Fig. 7. Drop-casting of GO on stainless steel current collectors

D. Synthesis of electrolyte

The hydrogel polymer electrolyte was made using poly (vinyl alcohol) (PVA) as a host matrix, water as a plasticizer, and phosphoric acid (H_3PO_4) as the electrolyte solution. The preparation of the hydrogel polymer electrolyte began with mixing with a magnetic stirrer, 1 g of PVA powder, and 10 ml of deionised water into a 50 ml beaker [35] [36]. The mixture was then heated up to ~80 °C until it turned from white to transparent. This solution was cooled down to 50 °C and then 0.03 mol (2.94 g) of H_3PO_4 electrolyte was added to the solution. The viscous solution was mixed thoroughly for one hour. After that, the clear, viscous solution was drop-cast into a glass Petri dish left overnight in the air to allow the excess water to evaporate.

Previous research has shown the capacitance properties increase as H_3PO_4 electrolyte concentration increases in the range 0.01 mol to 0.09 mol and became steady from 0.09 mol to 0.15 mol [36]. During synthesis of electrolyte in this research, we had found that at low concentration (0.01 mol to 0.02 mol) the electrolyte consistency was too stiff to practically work with; and at high concentrations (0.04 mol to 0.09 mol), the electrolyte consistency was too "runny". At 0.03 mol concentration, the electrolyte gel had a suitable gel consistency and fell in the applicable electrolyte concentration range [36].

E. Assembly of GO supercapacitor

PVA gel electrolyte is applied to the GO coated electrodes. The electrodes are then sandwiched together using a die-press that was manufactured from soft steel, as seen in Fig. 9. A pressure of ~1 MPa was applied to encapsulate the supercapacitor structure. A load of 90 kg was used to achieve this pressure.

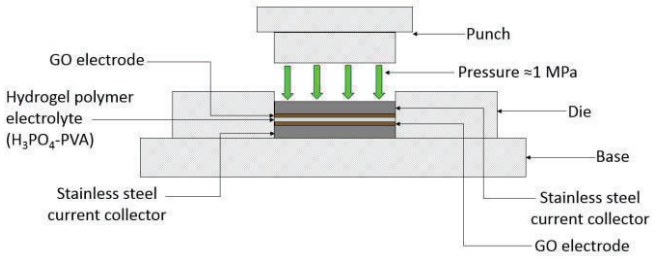

Fig. 8. Soft steel die-press sandwiching electrodes

F. GO characterisation

The morphology of the GO samples was characterized using High-Resolution Transmission Electron Microscopy (HRTEM). Elemental analysis was used to determine the carbon (C), hydrogen (H), sulphur (S), nitrogen (N), and oxygen (O) content in each GO sample. The chemical bonds in the graphite precursors and GO samples were determined by Fourier Transform Infrared (FTIR) spectroscopy.

The structure of the graphite precursors and GO samples were characterized by Raman spectroscopy at laser line wavelength of 514 nm. The intensities, full width at half maximum (FWHM), positions and integrated areas of the D band (I_D), G band (I_G), and 2D band (I_{2D}) were measured on the Raman spectrum for each sample. The ratio of I_D, and I_G (I_D/I_G) gives the degree of disorder or number of defects in the graphite and GO structure. The estimated crystallite size is determined from the Raman spectrum using (1) [37].

$$L_a = (2.4 \times 10^{-10})\lambda_l{}^4 \left(\frac{A_D}{A_G}\right)^{-1} \quad (1)$$

where,

- L_a = Estimated Crystallite size (nm)
- λ_l = Laser line wavelength (nm)
- A_D = Integrated intensity (area) of D band
- A_G = Integrated intensity (area) of G band.

The Raman spectra were baseline corrected by subtracting the baseline with baseline mode asymmetric least squares smoothing. Fitting of the Raman spectra was attained using the multi-peak Gaussian method by (2) for two peaks. Scaling was done by Levenberg-Marquardt algorithm with a tolerance of 0.0001.

$$y = y_0 + \left(\sqrt{\frac{2}{\pi}} \times \frac{A_1}{w_1} \times e^{-2\times\frac{(x-x_{c1})^2}{{w_1}^2}}\right) + \left(\sqrt{\frac{2}{\pi}} \times \frac{A_2}{w_2} \times e^{-2\times\frac{(x-x_{c2})^2}{{w_2}^2}}\right) \quad (2)$$

where,

- A1 = Area of First Peak
- w1 = Width of First Peak
- x_{c1} = Centre of First of Peak
- A2 = Area of Second Peak
- w2 = Width of Second Peak
- x_{c2} = Centre of Second of Peak.

G. GO supercapacitor electrochemical measurement

CV was performed on the GO samples using a three-electrode system at typical scan rates [38] [39] of 10 $mV.s^{-1}$, 20 $mV.s^{-1}$, and 100 $mV.s^{-1}$. Since the electrolyte is inorganic and comprises of water (H_2O) which splits into hydrogen (H_2) and oxygen (O_2) gases at a voltage of 1.23 V, the supercapacitor was operated between 0 V and 1 V to avoid decomposition of the electrolyte.

To evaluate the energy storage capabilities, gravimetric (per mass) capacitance can be calculated using (3).

$$C = \frac{\int_{E_1}^{E_2} i(E)dE}{2\nu m(E_2 - E_1)} \quad (3)$$

where,

- $\int_{E_1}^{E_2} i(E)dE$ = Total Voltammetric Charge
- E_1 = Low Potential Limit (V)
- E_2 = High Potentials Limit (V)
- ν = Scan Rate ($V.s^{-1}$)
- m = Active Mass of the Sample GO (g).

Energy density was calculated using (4).

$$E = \frac{1}{2}CV^2 \quad (4)$$

where,

- E = Energy density ($J.g^{-1}$)
- C = Specific Gravimetric Capacitance ($F.g^{-1}$)
- V = Potential Difference (V)

IV. Results and Discussion

The circular holes in Fig. 9 are the holes in the carbon grid. In all samples, a sheet-like structure is seen, which is typical of GO. Another critical characteristic of GO is its minimal thickness regarded as 2D. All samples are highly transparent in the HRTEM images showing that the GO is exceptionally thin.

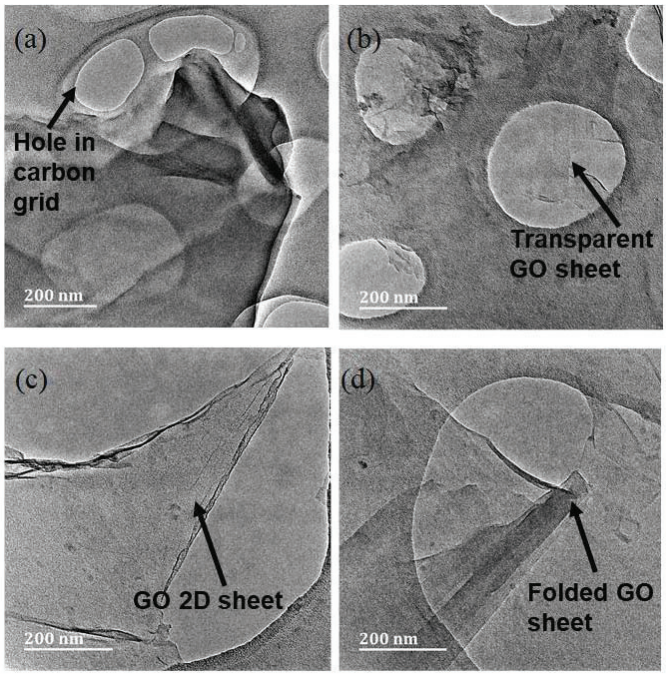

Fig. 9. HRTEM of (a) AN1-GO, (b) AN2-GO, (c) AN3-GO, (d) AN4-GO

The graphite precursors had some impurities of oxygen, sulphur, and nitrogen as seen in the elemental results shown in Table I. These impurities are inherent in natural occurring graphite. AN1-GO sample has the highest oxygen content as compared to the other GO samples as seen in Table I. This means that AN1-GO had achieved the highest oxidation and therefore had a more significant number of oxygen functional groups than the other GO samples. This result was expected since AN1-GO was produced using natural graphite precursor with the smallest flake size (0.045 mm).

There is a trend with the GO samples where the increase in flake size of their graphite precursor increases sulphur content. Sulphur has been shown to increase capacitance in supercapacitors by enhancing conductivity, wettability and overall performance [40] [41] [42].

TABLE I
Elemental Analysis Results

Sample	C (%)	O (%)	S (%)	N (%)	H (%)
AN1-Graphite	97.180	1.139	1.268	0.413	0.000
AN2-Graphite	93.815	1.182	1.127	3.876	0.000
AN3-Graphite	94.297	1.112	0.994	3.597	0.000
AN4-Graphite	95.342	0.925	0.145	3.588	0.000
AN1-GO	41.80	53.095	1.881	0.05	3.174
AN2-GO	57.91	35.733	3.314	0.01	3.033
AN3-GO	61.63	30.573	4.576	0.01	3.211
AN4-GO	58.98	32.699	5.213	0.00	3.108

In order to confirm oxidation was not affected by flake size, FTIR analysis was conducted on the smallest (AN1) and largest (AN4) flake sizes. In Fig. 10, the FTIR spectra of AN1-Graphite and AN4-Graphite has a noticeable variation. The significant variation is that the O–H bond of AN4-Graphite sample is broader (3700 cm^{-1} to 2200 cm^{-1}) than AN1-Graphite (3700 cm^{-1} to 3000 cm^{-1}). This bond is attributed to the water that naturally occurs in graphite. Therefore, it can be deduced that the large flake sized (0.450 mm) graphite precursor has more water content than the small flake sized (0.045 mm) graphite precursor. The vibration mode of C–H bonds at 2934 cm^{-1} and 2860 cm^{-1} are attributed by the aldehyde functional group are seen in AN1-Graphite sample but not in AN4-Graphite sample.

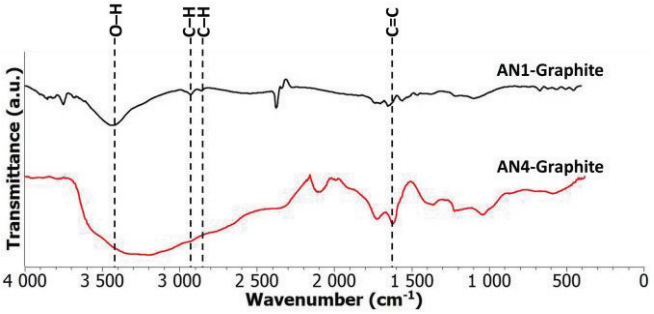

Fig. 10. FTIR spectra of AN1-Graphite and AN4-Graphite

In Fig. 11, a broad O–H is seen for AN1-GO. This result means that after synthesis, AN1-GO was significantly oxidized. This observation agrees with the elemental analysis results of AN1-GO having a high oxygen content. AN1-GO, and AN4-GO have similar FTIR spectra with AN1-GO with

marginally broader peak for the O–H bond as seen in Fig. 11. The bonds C=O (1880 cm^{-1} to 1680 cm^{-1}), C=C (1680 cm^{-1} to 1500 cm^{-1}), and C–O (1150 cm^{-1} to 890 cm^{-1}) are attributed to the vibration modes of ketonic, sp2-hybridized aromatic, and ether more specific epoxide species respectively.

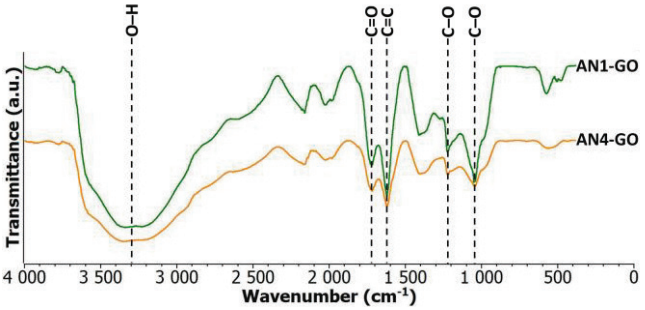

Fig. 11. FTIR spectra of AN1-GO and AN4-GO

The results obtained from the Raman spectra for graphite precursors are shown in Table II. Raman spectra for natural graphite precursor samples shows two prominent bands i.e., the G band, and 2D band, as seen in Fig. 12. The G band is attributed to vibration of the sp2 hybridization in the graphitic structure.

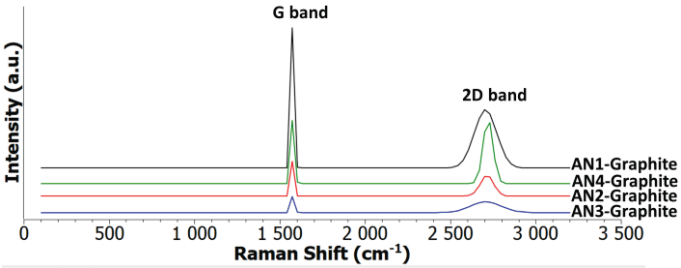

Fig. 12. Raman spectra of graphite precursors

The D band was not observed for graphite precursors therefore their crystallite sizes were not estimated, and disorder could not be determined. The D band is due to out of plane vibration caused by defects in the graphitic structure. This factor does not mean that the natural graphite precursors' structure had no defects but minute defects that can be negligible. These minor defects could be from the little oxygen, sulphur and nitrogen content in the graphite precursors, as shown in Table I.

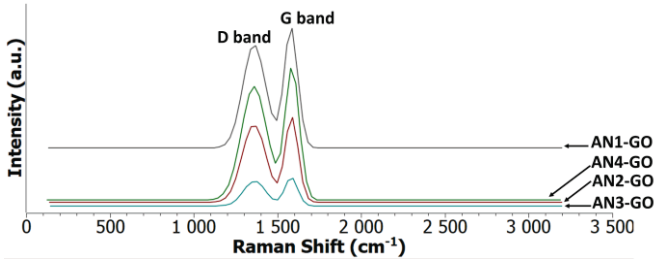

Fig. 13. Raman spectra of GO samples

In Fig. 13, the Raman spectra for GO samples showed only D band, and G band with no 2D band being observed. GO samples show a high amount of defects, as seen in Table III with the average I_D/I_G ratio of 0.87. The defects are due to sp3 hybridization caused by oxygen functional groups. The crystallite sizes are relatively small, with an average of 11.11 nm. This result means that GO produced from natural graphite has low crystallinity.

TABLE II
RAMAN RESULTS FOR GRAPHITE PRECURSORS

SAMPLES		AN1-Graphite	AN2-Graphite	AN3-Graphite	AN4-Graphite
G BAND	POSITION	1575.17	1579.24	1581.74	1581.74
	FWHM	17.52	16.03	14.94	14.71
2D BAND	POSITION	2705.84	2714.68	2707.58	2720.58
	FWHM	130.44	78.08	178.67	58.18

TABLE III
RAMAN RESULTS FOR GO SAMPLES

SAMPLES		AN1-GO	AN2-GO	AN3-GO	AN4-GO
D BAND	POSITION	1361.13	1359.51	1362.82	1360.57
	FWHM	135.64	141.61	130.02	153.16
G BAND	POSITION	1580.64	1585.00	1582.05	1588.14
	FWHM	20.68	24.47	17.38	21.37
I_D/I_G		0.85	0.91	0.87	0.86
L_A (nm)		11.63	10.33	11.63	10.84

The cyclic voltammograms of the GO samples are shown in Fig. 14, Fig. 15, and Fig. 16.

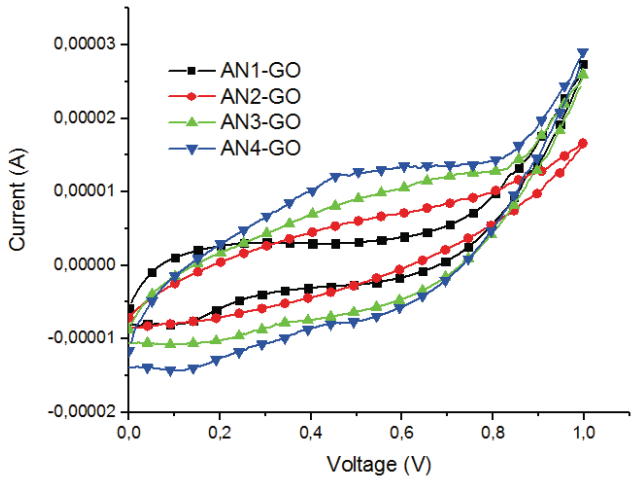

Fig. 14. CV curves for GO samples at 10 $mV.s^{-1}$ scan rate

Fig. 14 shows a nearly symmetric curve for all samples showing a typical electrical double layer capacitive behavior. Even at a high scan rate of 100 $mV.s^{-1}$, a similar shape is seen for the CV curves as seen in Fig. 16.

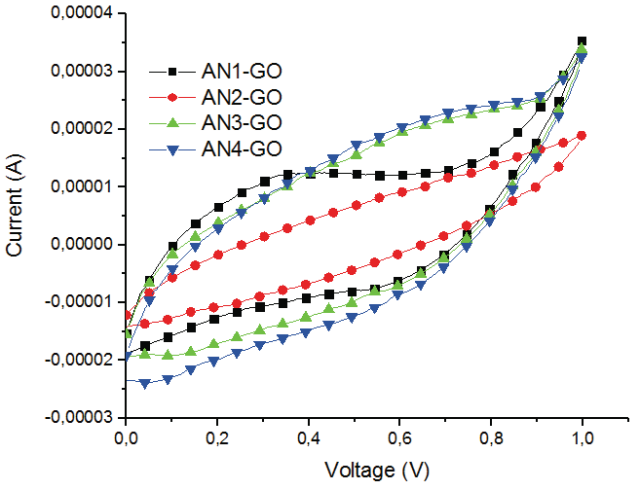

Fig. 15. CV curves for GO samples at 20 mV.s^{-1}

The gravimetric capacitances for each sample were calculated from the CV curves. AN4-GO has the highest specific gravimetric capacitance of 204.22 F.g^{-1} at a scan rate of 10 mV.s^{-1} almost four times higher than AN1-GO as shown in Fig. 17.

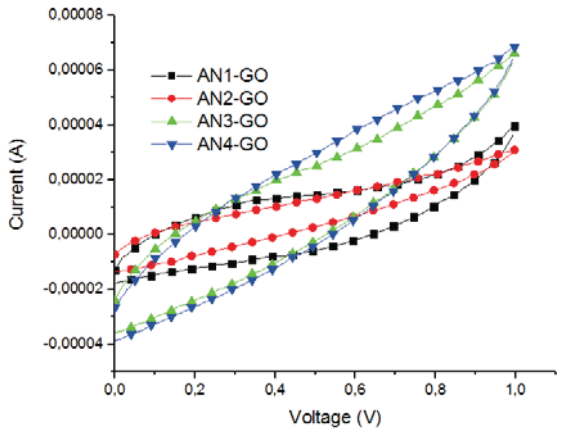

Fig. 16. CV curves for GO samples at 100 mV.s^{-1}

AN4-GO specific gravimetric capacitance is of similar order of magnitude than ultrahigh-level functionalized graphene supercapacitor [43]. AN4-GO had a specific gravimetric capacitance, almost double compared to nitrogen doped carbon aerogel supercapacitor's specific gravimetric capacitance of 115 F.g^{-1} [44].

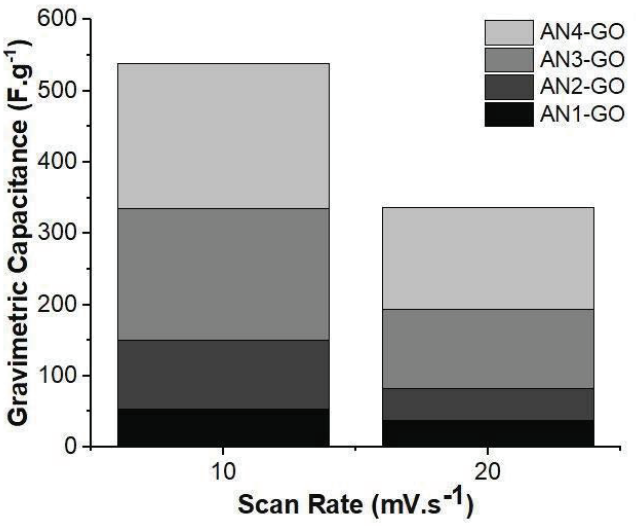

Fig. 17. Gravimetric Capacitance vs. Scan Rate CV

AN1-GO having higher oxygen content does not have higher capacitance as expected due to more pseudocapacitance effect. It is the changing of particle size of the precursor graphite that influences the capacitance of the GO produced, as seen in Fig. 19.

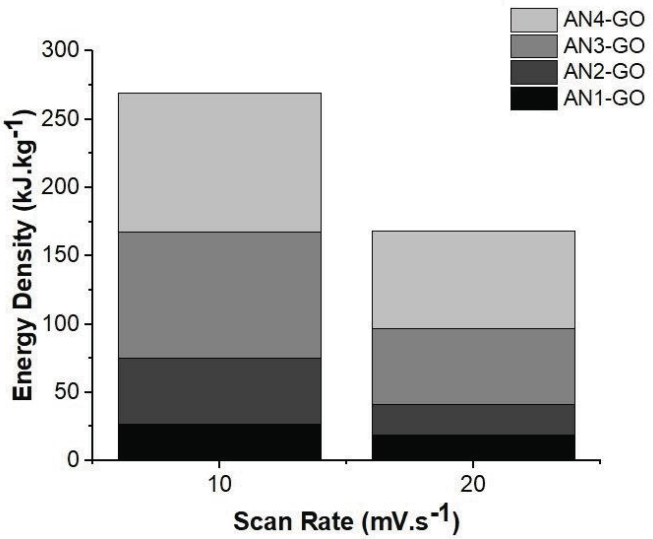

Fig. 18. Energy Density vs. Scan Rate

The average particle size from 0.0405 mm to 0.1250 mm has a steep almost linear increase in the specific capacitance, but from 0.1250 mm to 0.4500 mm there is a gradual increase in specific capacitance suggesting there is a limiting point for the average particle size.

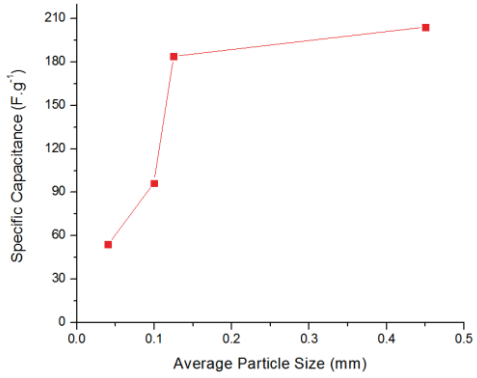

Fig. 19. Specific capacitance as a function of average particle size at scan rate 10 mV.s^{-1}

Fig. 20 shows the specific capacitance as a function of the scan rate. It is clear that the specific capacitance values of AN4-GO are higher than those of all other samples at scan rates 10 mV.s^{-1}, and 20 mV.s^{-1}. AN4-GO produced from graphite precursor with the larger flake size has the highest energy density of 102.11 kJ.kg^{-1} as shown in Fig. 18 meaning it is more suitable for energy storage application. This energy density achieved, is much higher than energy density of commercially available carbon-based supercapacitors of 18 kJ.kg^{-1} [45]. The energy density of AN4-GO is almost five times greater than supercapacitors compared to other recent developments in supercapacitor research [43] [46] [47].

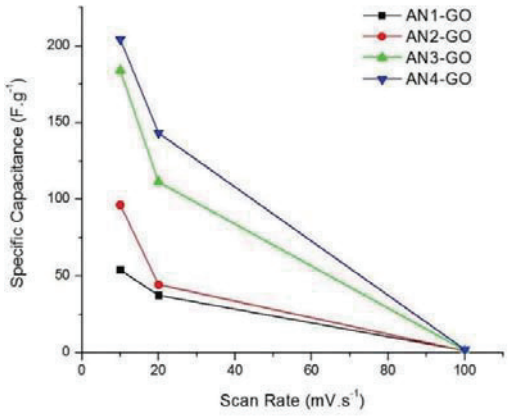

Fig. 20. Specific capacitance as a function of the scan rate

V. Conclusion

We found that, in the particle size range 0.0405 mm to 0.4500 mm, GO produced from smaller flake size (0.0405 mm) graphite precursor, has a more significant amount of oxygen functional groups, and lower capacitance than larger flake size (0.4500 mm) based GO. This observation implies that the pseudocapacitance effect does not have a significant impact on GO.

The energy density of GO samples synthesized from graphite precursor of a larger flake size is higher than GO synthesized from a smaller flake size graphite precursor, thus making it the preferred flake size when fabricating GO electrodes for supercapacitors for energy storage applications.

References

[1] R. Inglesi, "Aggregate electricty demand in South Africa: Conditional forecasts 2030," *Applied Energy,* vol. 87, pp. 197-204, 2010.

[2] S.SA, "Energy and the poor: a municipal breakdown," 4 June 2018. [Online]. Available: http://www.statssa.gov.za/p=11181. [Accessed 24 2019 July].

[3] H. Yang, "A Review of Supercapacitor-based Energy Storage Systems for Microgrid Applications," in *IEEE Power & Energy Society General Meeting (PESGM)*, Portland, 2018.

[4] B. Xu, H. Wang, Q. Zhu, N. Sun, B. Anasori, L. Hu, F. Wang, Y. Guan and Y. Gogotsi, "Reduced graphene oxide as a multi-functional conductive binder for supercapacitor electrodes," *Energy Storage Materials,* vol. 12, pp. 128-136, 2018.

[5] C.V.V.M. Gopi and H.-J. Kim, "Design of Supercapacitor for Electric and Hybrid Vehicles : Supercapacitor," in *International Conference on Information and Communication Technology Robotics (ICT-ROBOT)*, Busan, 2018.

[6] W. Ma, S. Chen, S. Yang, W. Chen, W. Weng, Y. Cheng and M. Zhu, "Flexible all-solid-state asymmetric supercapacitor based on transition metal oxide nanorods/reduced graphene oxide hybrid fibers with high energy density," *Carbon,* vol. 113, pp. 151-158, 2017.

[7] M. Ye, J. Gao, Y. Xiao, T. Xu, Y. Zhao and L. Qu, "Metal/graphene oxide batteries," *Carbon,* vol. 125, pp. 299-307, 2017.

[8] J.-Q. Huang, T.-Z. Zhuang, Q. Zhang, H.-J. Peng, C.-M. Chen and F. Wei, "Permselective Graphene Oxide Membrane for Highly Stable and Anti-Self-Discharge Lithium–Sulfur Batteries," *ACS Nano,* vol. 9, no. 3, pp. 3002-3011, 2015.

[9] K. Fu, Y. Wang, C. Yan, Y. Yao, Y. Chen, J. Dai, S. Lacey, Y. Wang, J. Wan, T. Li, Z. Wang, Y. Xu and L. Hu, " Graphene Oxide-Based Electrode Inks for 3D-Printed Lithium-Ion Batteries," *Advanced Materials,* vol. 28, p. 2587–2594, 2016.

[10] C. Kim, J. W. Kim, H. Kim, D. H. Kim, C. Choi, Y. S. Jung and J. Park, "Graphene Oxide Assisted Synthesis of Self-assembled Zinc Oxide for Lithium-Ion Battery Anode," *Chemistry of Materials,* vol. 28, no. 23, p. 8498–8503, 2016.

[11] Y. Jiang, F. Chen, Y. Gao, Y. Wang, S. Wang, Q. Gao, Z. Jiao, B. Zhao and Z. Chen, "Inhibiting the shuttle effect of Li–S battery with a graphene oxide coating separator: Performance improvement and mechanism study," *Journal of Power Sources,* vol. 342, pp. 929-938, 2017.

[12] S. Yuan, Z. Guo, L. Wang, S. Hu, Y. Wang and Y. Xia, "Leaf-Like Graphene-Oxide-Wrapped Sulfur for High-Performance Lithium–Sulfur Battery," *Advanced Science,* vol. 2, pp. 1-10, 2015.

[13] B. Xu, S. Yue, Z. Sui, X. Zhang, S. Hou, G. Caoa and Y.Yang, "What is the choice for supercapacitors: graphene and graphene oxide?," *Energy & Environmental Science,* no. 4, pp. 2826-2830, 2011.

[14] S. Korkmaz and A. Kariper, "Graphene and graphene oxide based aerogels: Synthesis, characteristics and supercapacitor applications," *Journal of Energy Storage,* vol. 27, pp. 1-12, 2020.

[15] M. Down, S. J. Rowley-Neale, G. Smith and C. E. Banks, "Fabrication of Graphene Oxide Supercapacitor Devices," *ACS Applied Energy Materials,* vol. 1, no. 2, pp. 707-714, 2018.

[16] H. Xian, T. Peng and H. Sun, "Effect of Particle Size of Natural Garphite on the Size and Structure of Graphene Oxide Prepared by the Modified Hummers Method," *Materials Science Forum,* vol. 814, pp. 185-190, 2015.

[17] D. R. Chowdhury, C. Singh and A. Paul, "Role of graphite precursor and sodium nitrate in graphite oxide synthesis," *RSC Advances,* no. 29, pp. 15138-15145, 2014.

[18] A. S. Aricò, P. Bruce, B. Scrosati, J.-M. Tarascon and W. V. Schalkwijk, "Nanostructured materials for advanced energy conversion and storage devices," *Nature Materials,* vol. 4, pp. 366-377, 2005.

[19] R.Kötz and M.Carlen, "Principles and applications of electrochemical capacitors," *Electrochimica Acta,* vol. 45, no. 15-16, pp. 2483-2498, 2000.

[20] B. E. Conway, Electrochemical Supercapacitors, Scientific Fundamentals and Technological Applications, New York: Kulwer Academic/Plenum Publishers, 1999.

[21] Y. Li, M. V. Zijil, S. Chiang and N. Pan, "KOH modified graphene nanosheets for supercapacitor electrodes," *Journal of Power Sources,* vol. 196, no. 14, pp. 6003-6006, 2011.

[22] W. K. Chee, H. N. Lim, Z. Zainal, N. M. Huang, I. Harrison and Y. Andou, "Flexible Graphene-Based Supercapacitors: A Review," *The Journal of Physical Chemistry C,* vol. 120, no. 8, pp. 4153-4172, 2016.

[23] L. Gouy, "Constitution of the electric charge at the surface of an electrolyte," *Journal of Physical Theory and Applications,* vol. 9, pp. 457-468, 1910.

[24] D. Chapman, "A contribution to the theory of electrocapillarity," *Philosophical Magazine Series 6,* vol. 25, pp. 475-481, 1913.

[25] J. O. Bockris, M. Devanathan and K. Muller, "On the Structure of Charged Interfaces," in *Royal Society of London. Series A. Mathematical and Physical Sciences*, London, 1963.

[26] W. Pell and B. Conway, "Voltammetry at a de Levie brush electrode as a model for electrochemical supercapacitor behaviour," *Journal of Electroanalytical Chemistry,* vol. 500, no. 1-2, pp. 121-133, 2001.

[27] F. Beguin and E. Frackowiak, Supercapacitors: Materials, Systems and Applications, Germany: Wiley-VCH Verlag GmbH & Co. KGaA, 2013.

[28] J. G. S. Moo, B. Khezri, R. D. Webster and M. Pumera, "Graphene Oxides Prepared by Hummers', Hofmann's, and Staudenmaier's Methods: Dramatic Influences on Heavy-Metal-Ion Adsorption," *ChemPhysChem,* vol. 15, no. 14, pp. 2922-2929, 2014.

[29] D. A. Dikin, S. Stankovich, E. J. Zimney, R. D. Piner, G. H. B. Dommett, G. Evmenenko, S. T. Nguyen and R. S. Ruoff, "Preparation and characterization of graphene oxide paper," *Nature,* vol. 448, p. 457–460, 2007.

[30] J. Tian, S. Wu, X. Yin and W. Wu, "Novel preparation of hydrophilic graphene/graphene oxide nanosheets for," *Applied Surface Science,* vol. 496, no. 143696, pp. 1-11, 2019.

[31] C. Botas, P. Álvarez, C. Blanco, R. Santamaría, M. Granda, P. Ares, F. Rodríguez-Reinoso and R. Menéndez, "The effect of the parent graphite on the structure of graphene oxide," *Carbon,* vol. 50, no. 1, pp. 275-282, 2012.

[32] D. C. Marcano, D. V. Kosynkin, J. M. Berlin, A. Sinitskii, Z. Sun, A. Slesarev, L. B. Alemany, W. Lu and J. M. Tour, "Improved Synthesis of Graphene Oxide," *ACS Nano,* vol. 4, no. 8, pp. 4806-4814, 2010.

[33] I.-L. Tsai, J. Cao, L. L. Fevre, B. Wang, R. Todd, R. A. Dryfe and A. J.Forsyth, "Graphene-enhanced electrodes for scalable supercapacitors," *Electrochimica Acta,* vol. 257, pp. 372-379, 2017.

[34] A. Y. S. Eng, C. Kiang and C. M. Pumera, "Intrinsic electrochemical performance and precise control of surface porosity of graphene-modified electrodes using the drop-casting technique," *Electrochemistry Communications,* vol. 59, pp. 86-90, 2015.

[35] M. Kaempgen, C. K. Chan, J. Ma, Y. Cui and G. Gruner, "Printable Thin Film Supercapacitors Using Single-Walled Carbon Nanotubes," *Nano Letters,* vol. 9, no. 5, pp. 1872-1876, 2009.

[36] Q. Chen, X. Li, X. Zang, Y. Cao, Y. He, P. Li, K. Wang, J. Wei, D. Wu and H. Zhu, "Effect of different gel electrolytes on graphene-based solid-state supercapacitors," *RSC Advances,* vol. 4, no. 68, pp. 36253-36256, 2014.

[37] L. G. Cançadoa, K. Takai, T. Enoki, M. Endo, Y. A. Kim, H. Mizusaki, A. Jorio, L. N. Coelho, R. Magalhães-Paniago and M. A. Pimenta, "General equation for the determination of the crystallite size La of nanographite by Raman spectroscopy," *Applied Physics Letters,* vol. 88, no. 16, pp. 1-3, 2006.

[38] Q. Li, X. Guo, Y. Zhang, W. Zhang, C. Ge, L. Zhao, X. Wang, H. Zhang, J. Chen, Z. Wang and L. Sun, "Porous graphene paper for supercapacitor applications," *Journal of Materials Science & Technology,* vol. 33, no. 8, pp. 793-799, 2017.

[39] J. Yu, M. Wang, P. Xu, S.-H. Cho, J. Suhr, K. Gong, L. Meng, Y. Huang, J.-H. Byun, Y. Oh, Y. Yan and T.-W. Chou, "Ultrahigh-rate wire-shaped supercapacitor based on graphene fiber," *Carbon,* vol. 119, pp. 332-338, 2017.

[40] Y. Zhou, S. L. Candelaria, Q. Liu, Y. Huang, E. Uchaker and G. CaO, "Sulfur-rich carbon cryogels for supercapacitors with improved conductivity and wettability," *Journal of Materials Chemistry A,* vol. 2, no. 22, pp. 8472-8482, 2014.

[41] Y. Zhou, R. Ma, S. L.Candelaria, J. Wang, Q. Liu, E. Uchaker, P. Li, Y. Chen and G. Cao, "Phosphorus/sulfur Co-doped porous carbon with enhanced specific capacitance for supercapacitor and improved catalytic activity for oxygen reduction reaction," *Journal of Power Sources,* vol. 314, pp. 39-48, 2016.

[42] X. Yu, Y. Kang and H. S. Park, "Sulfur and phosphorus co-doping of hierarchically porous graphene aerogels for enhancing supercapacitor performance," *Carbon,* vol. 101, pp. 49-56, 2016.

[43] Z. Li, S. Gadipelli, Y. Yang, G. He, J. Guo, J. Li, Y. Lu, C. A. Howard, D. J. Brett, I. P. Parkin, F. Li and Z. Guo, "Exceptional supercapacitor performance from optimized oxidation of graphene-oxide," *Energy Storage Materials,* vol. 17, pp. 12-21, 2019.

[44] F.-Y. Zeng, Z.-Y. Su, S. Liu, H.-P. Liang, H.-H. Zha and B.-H. Han, "Nitrogen-doped carbon aerogels with high surface area for supercapacitors and gas adsorption," *Materials Today Communications,* vol. 16, pp. 1-7, 2018.

[45] J. Xu, Z. Tan, W. Zeng, G. Chen, S. Wu, Y. Zhao, K. Ni, Z. Tao, M. Ikram, H. Ji and Y. Zhu, "A Hierarchical Carbon Derived from Sponge-Templated Activation of Graphene Oxide for High-Performance Supercapacitor Electrodes," *Advanced Materials,* vol. 28, no. 26, pp. 5222-5228, 2016.

[46] Z. Lei, J. Zhang, L. L. Zhang, N. A. Kumar and X. S. Zhao, "Functionalization of chemically derived graphene for improving its electrocapacitive energy storage properties," *Energy & Environmental Science,* vol. 9, no. 6, pp. 1891-1930, 2016.

[47] R. Raccichini, A. Varzi, S. Passerini and B. Scrosati, "The role of graphene for electrochemical energy storage," *Nature Materials,* vol. 14, p. 271–279, 2015.

S. Perumal, born on 20 July 1995, in Chatsworth, Durban, KwaZulu-Natal, South Africa, received his BSc Degree in Electrical Engineering in the year 2017, and MSc Degree in Electrical Engineering in the year 2020 from the University of KwaZulu-Natal in Durban, KwaZulu-Natal, South Africa. He aspires to pursue his Ph.D. Degree in Electrical Engineering.

From 2019 to 2020, he was a Junior Electrical Engineer. In 2020, he was an assistant lecturer. He is currently an Electrical Engineer in the Smart Grid Research Centre under the Eskom Power Plant Engineering Institute at University of KwaZulu-Natal. His research interests include graphene and graphene oxide-related materials in high voltage and energy storage applications.

Mr. Perumal is a candidate engineer under Engineering Council of South Africa (ECSA) as well as a member of IEEE-Eta Kappa Nu Honor Society.

A.L.L. Jarvis received a B.Sc. Degree in Electronic Engineering from the University of Natal, Durban, KwaZulu-Natal, South Africa, in the year 1992, and a Ph.D. Degree in Electronic Engineering from the University of KwaZulu-Natal, Durban, KwaZulu-Natal, South Africa, in the year

He is the current Director of a research centre that falls under the Eskom Power Plant Engineering Institute. He has received a number of research grants from chemical and power utility industries. His research interests fall broadly in materials science with a focus on carbon-based nanotechnology and high temperature superconductors.

Dr. Jarvis is a member of the South African Institute of Electrical Engineers (SAIEE).

M. Z. Gaffoor received his BSc Degree in Electronic Engineering from University of KwaZulu-Natal, Durban, KwaZulu-Natal, South Africa, in the year 2017 and his MSc Degree in Electronic Engineering from University of KwaZulu-Natal, Durban, KwaZulu-Natal, South Africa in the year 2019. He is currently pursuing a Ph.D. Degree in Electronic Engineering at University of KwaZulu-Natal, Durban, KwaZulu-Natal, South Africa.

He is currently an electronic design engineer at Synap Labs His research interests include synthesis and applications of graphene-based materials and high temperature superconductors.

Mr. Gaffoor is registered as a candidate engineer with the Engineering Council of South Africa (ECSA).

CONTENTS PAGE